

Analytical Modelling of Near-Field Coupling Communication between Persons Equipped with Wearable Terminals through Handshaking

Ryo Takeuchi
Kyoto Institute of Technology
Matsugasaki Sakyo - ku
Kyoto, Japan

Shin Hasegawa
Kyoto Institute of Technology
Matsugasaki Sakyo - ku
Kyoto, Japan

Yuichi Kado
Kyoto Institute of Technology
Matsugasaki Sakyo - ku
Kyoto, Japan
kado@kit.ac.jp

Daiki Ayuzawa
Hosei University
3-7-2, Kajino-cho, Koganei-shi
Tokyo, Japan

Mitsuru Shinagawa
Hosei University
3-7-2, Kajino-cho, Koganei-shi
Tokyo, Japan
m.shina@hosei.ac.jp

Kyoji Ohashi
Nippon Signal Company
11-2, Hiraidekogyodanchi
Utsunomiya-shi, Tochigi, Japan

Daisuke Saito
Nippon Signal Company
11-2, Hiraidekogyodanchi
Utsunomiya-shi, Tochigi, Japan

ABSTRACT

Near-field coupling communication (NFCC) is a communication technology that treats the surface of the human body as a transmission path using a carrier frequency below 10 MHz. Because the radiation signal to a space is suppressed in NFCC, humans wearing an NFCC transceiver (TRX) can exchange personal information through handshaking without having to worry about information leakage. This work examines the mechanism of communication between wearable transceivers by NFCC through handshaking and the requirements for stable handshaking communication. The establishment of handshaking communication requires the signal propagation loss in the handshaking posture to be at least 10 dB smaller than in the standing posture. Signal propagation losses in the standing and handshaking postures were measured with an electrically isolated probe when TRXs were attached to the front of two human bodies standing face to face 600 mm apart. We investigated a simulation model of handshaking communication using a phantom we developed instead of a real human body by electromagnetic simulation and circuit simulation. On the basis of the simulation results, we proposed the signal propagation path for the realization of handshaking communication. When wearable TRXs are inserted into the soles of shoes, the signal propagation path is satisfied. In this case, we experimentally confirmed that the signal propagation loss in handshaking is smaller than that in the standing posture by 10.6dB.

Categories and Subject Descriptors

B.4.1 [INPUT/OUTPUT AND DATA COMMUNICATIONS]:
Data Communications Devices – *Receivers, Transmitters.*

B.4.2 [INPUT/OUTPUT AND DATA COMMUNICATIONS]:
Input / Output Devices – *Channels and controllers*

General Terms

Measurement, Design, Reliability, Experimentation, Security, Human Factors, Standardization

Keywords

Near-field coupling communication (NFCC), Electrically isolated measurement, Human equivalent phantom, Signal propagation loss, Electrical-to-optical and optical-to-electrical measurement (E/O and O/E measurement).

1. INTRODUCTION

Near-field coupling communication (NFCC) is a communication technology that uses the surface of the human body as a transmission path since the signal loss propagating through the conductor surface is less than the signal loss propagating through the space by using a carrier frequency below 10 MHz [1]. The main advantages of NFCC are the short radial distance and the establishment of a “touch and connect” intuitive form of communication. Figure 1 shows examples of NFCC application. A person can walk through a ticket gate without bringing out a card device, and two persons can exchange electronic business cards by handshaking. They are wearing NFCC devices that can exchange personal information through handshaking without any concern for leakage of information. Communication by handshaking with TRX installed on the soles of shoes has been reported [2]. However, the mechanism and requirements to establish stable communication by NFCC through handshaking have not yet been clarified. This work examines the feasibility of communication between wearable transceivers by NFCC through handshaking. We call such communication “handshaking

communication". Signal propagation losses in the standing posture and handshaking posture were measured with an electrically isolated probe when TRXs were attached to the front of two human bodies facing each other. We investigated the simulation model of handshaking communication using our developed phantom instead of a real human body by electromagnetic simulation and circuit simulation. On the basis of experimental and simulated results, we came up with the signal propagation path for the establishment of handshaking communication.

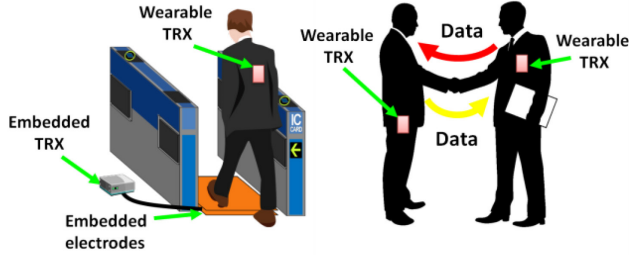


Figure 1. Hands-free ticket gate and handshaking communication systems using near-field coupling communication technology.

2. REQUIREMENTS FOR REALIZATION OF HANDSHAKING COMMUNICATION

Figure 2 shows a photograph of prototype TRX that we developed [3]. For realization of handshaking communication, signal propagation loss in the handshaking posture needs to be smaller than that in standing posture as shown in the Fig. 3. We need to consider the manufacturing variation of about 2 dB in TRX performance and the propagation loss variation of about 2 dB depending on human shape when we investigate the requirements for realization of handshaking communication. Since handshaking communication consist of two persons and two TRXs, we need to take into account the margin of 2 dB for the worst case when the performance variation between two TRXs is 4 dB ($2 \text{ dB} \times 2 \text{ TRXs}$) and the signal propagation loss variation regarding the human factor is 4 dB ($2 \text{ dB} \times 2 \text{ persons}$). Therefore, we set the first requirement as a value of 10 dB (the margin of $2 \text{ dB} + 4 \text{ dB} + 4 \text{ dB}$) for the signal propagation difference between standing and handshaking posture. Furthermore, we set the second requirement as a 20 dB or higher S/N ratio for the communication system in the handshaking posture when handshaking communication uses the prototype TRX that we developed. In this paper, we discussed first requirement.

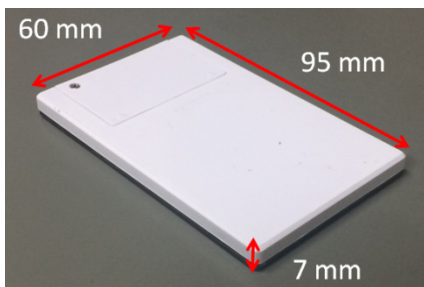


Figure 2. Photograph of prototype TRX.

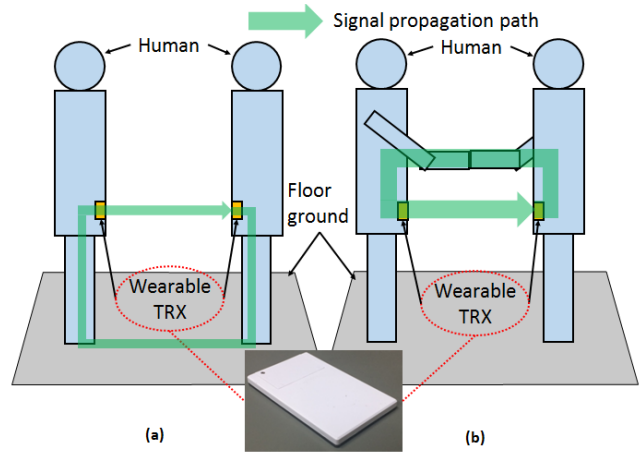


Figure 3. Signal propagation path in (a) standing posture and (b) handshaking posture.

3. MEASUREMENT TOOL

3.1 Battery-powered Transmitter

We developed a battery-powered transmitter (TX) to reduce the signal propagation path enhancement by electrically connecting to a signal generator [4, 5]. The battery-powered TX includes a direct digital synthesizer (DDS) oscillator. It generates a sinusoidal wave. Figure 4 (a), (b), and (c) shows the internal circuits, a block diagram of the TX, and the external shape. To eliminate the effect of voltage drop in a lithium ion battery, we connected the battery to a regulator. The frequency of the sinusoidal wave can be modified from 50 Hz to 20 MHz in 1 Hz increments. The dimensions of the TX were $85 \times 62 \times 10 \text{ mm}$. The electrodes in the TX were $70 \times 50 \text{ mm}$ each. The signal voltage of the TX changes from 1 to $2 V_{p-p}$ when changing its frequency. The output impedance was 50Ω .

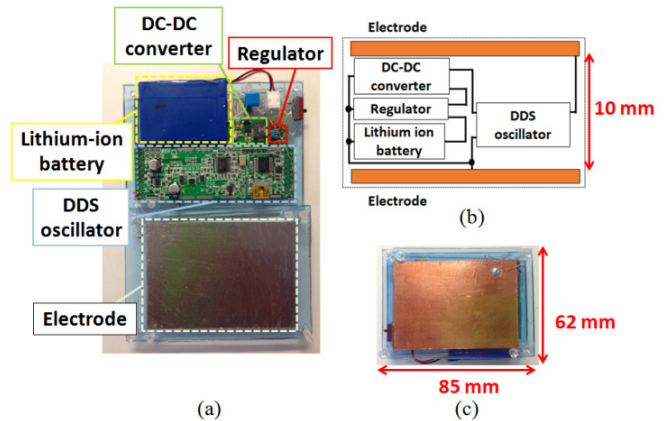


Figure 4. Battery-powered TX consisting of (a) internal circuit, (b) block diagram, and (c) external shape.

3.2 E/O-O/E Probe

Figure 5 (a) shows a photograph of the E/O-O/E probe. The probe has E/O and O/E conversion functions. A block diagram of the E/O probe is shown in Fig. 5 (b). The E/O converter consists of an E/O amplifier, peaking circuit, coupling capacitor, current source, and laser diode. The O/E converter consists of an O/E amplifier, peaking circuit, load resistor, and photodiode. The E/O converter receives the electrical signal, the E/O circuit converts the electrical signal into an optical signal, and the O/E circuit reconverts the optical signal into an electrical signal. These circuits enable the E/O converter to be electrically isolated from the measuring instrument. The circuit gain of the E/O-O/E probe is 71 dB at 6.75 MHz [6, 7].

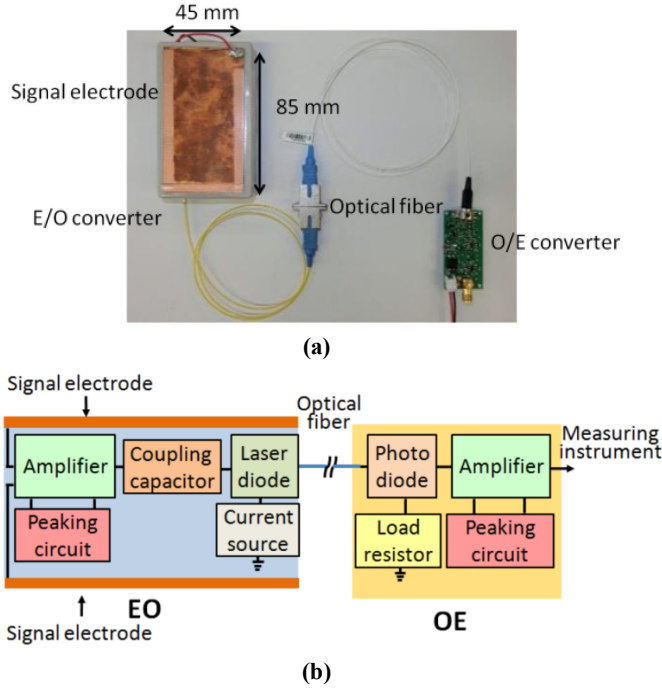


Figure 5. E/O-O/E probe: (a) external view and (b) block diagram.

4. MEASUREMENT SYSTEM AND RESULTS

We assumed a situation where two humans wearing a TRX stand face to face 600 mm apart and shake hands. The schematic of our experimental system is shown in Fig. 6. The height of the human was 170 cm. We used a battery-powered TX as a TX and an E/O-O/E probe as a receiver (RX). The battery-powered TX generates a sinusoidal wave at 6.75 MHz. The floor ground was measured to be 2000 × 3000 mm. The battery-powered TX and E/O-O/E probe were moved on the front of the human bodies. We measured the received voltage with the E/O-O/E probe while changing the distance between TRX and floor ground. We evaluated the signal propagation loss, which was represented by the ratio of the received voltage to the transmission voltage, defined as

$$\text{Signal propagation loss} = -20 \times \log_{10} \left\{ \frac{\text{Received voltage}}{\text{Transmitted voltage}} \right\} \quad (1)$$

Figure 7 shows the signal propagation losses that were calculated from the experimental results. A signal propagation loss difference of more than 10 dB between standing posture and handshaking posture is required for the establishment of handshaking communication. When the distance between TRX and floor ground was from 100 mm to 600 mm, the signal propagation loss differences were very small. When the distance between TRX and floor ground was from 600 mm to 1400 mm, the signal propagation losses of the handshaking posture were bigger than those of the standing posture. These results indicate that it is difficult to establish a handshaking communication system when the wearable TRXs are placed on the front of a human body.

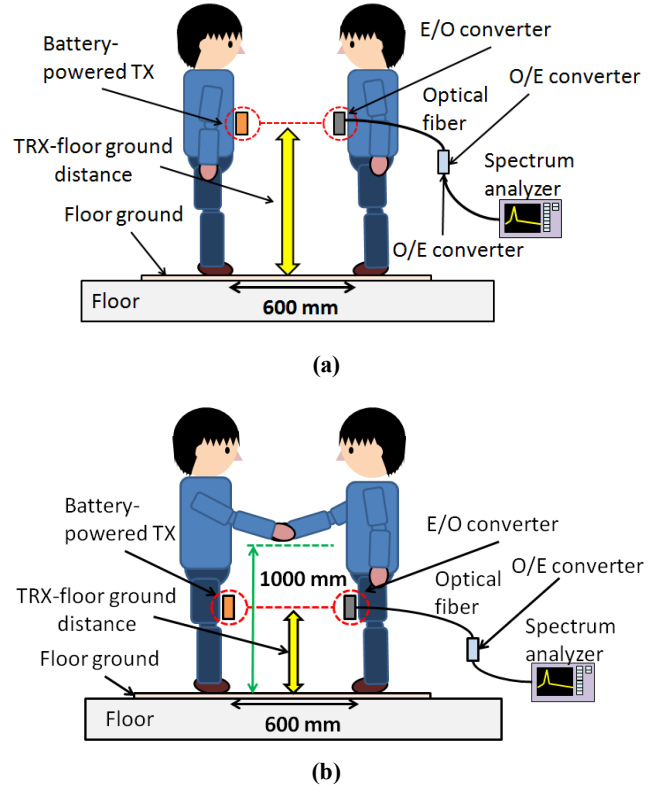


Figure 6. Measurement systems with (a) standing posture and (b) handshaking posture.

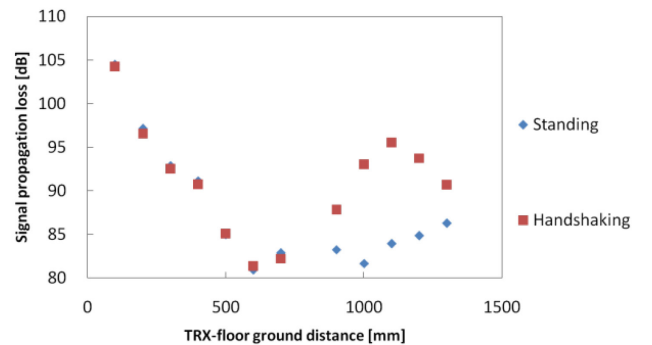


Figure 7. Dependence of signal propagation loss on distance between TRX and floor ground in experiment.

5. ANALYTICAL MODELLING OF NFCC

5.1 Model of Handshaking Communication Using Human Equivalent Phantom

We used phantoms having the same electrical characteristics as the human body in order to obtain reproductive results constantly [8]. Figure 8 shows a photograph of a phantom. Its outer shell is a polyvinyl chloride (PVC) pipe with a diameter of 250 mm, a thickness of 8 mm, and a height of 1800 mm. The pipe was filled with salt water, the conductivity of which was adjusted to 0.6 S/m at 6.75 MHz (human body: 0.6 S/m) [9]. The water level was 1500 mm. The relative permittivity of the water was 80.

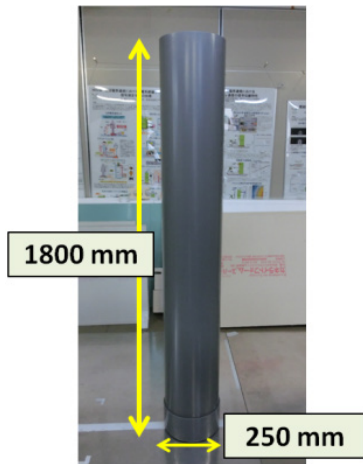


Figure 8. Photograph of human equivalent phantom.

The handshaking communication was modeled using the human body equivalent phantom in place of a real human body in the measurement system shown in Fig. 6 (a). We call this the “handshaking communication model”. Figure 9 shows the handshaking communication model. The model was composed of seven conductors (phantom 1 (no. 1) and a signal electrode 1 of the wearable TX (no. 2), a signal ground electrode 1 of the wearable TX (no. 3), a signal ground electrode 2 of the wearable RX (no. 4), a signal electrode 2 of the wearable RX (no. 5), phantom 2 (no. 6), and a floor ground (no.7)), as shown in Fig. 9.

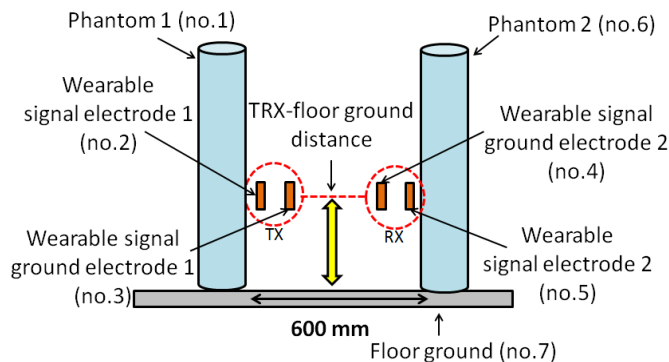


Figure 9. Handshaking communication model.

5.2 Equivalent Circuit Model of Handshaking Communication

An equivalent circuit of the handshaking communication model is represented by capacitances because conductors are capacitively coupled with each other in the NFCC system [10]-[12]. We calculated the capacitances between seven conductors with the 3D electromagnetic field simulator (Q3D Extractor) using a finite element method [13]. As shown in Fig. 10, these capacitances were applied to the lumped-parameter equivalent circuit for the handshaking communication model. The conductors shown in Fig. 9 are represented as nodes in the equivalent circuit. Figure 11 shows the simulation results of the capacitances as a function of the distance between TRX and floor ground in the standing postures. By substituting the capacitance in the equivalent circuit, signal propagation loss was calculated by a circuit simulator. Figure 12 shows the signal propagation loss of the handshaking communication model in the standing posture. The tendency of signal propagation loss by equivalent circuit was qualitatively similar to the tendency of the experimental results, which demonstrates that the handshaking communication model is valid.

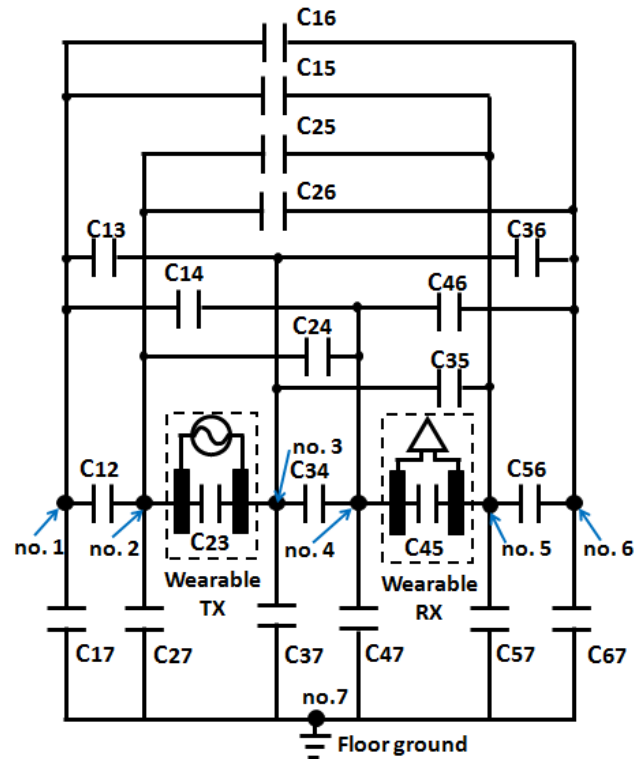


Figure 10. Lumped-parameter equivalent circuit.

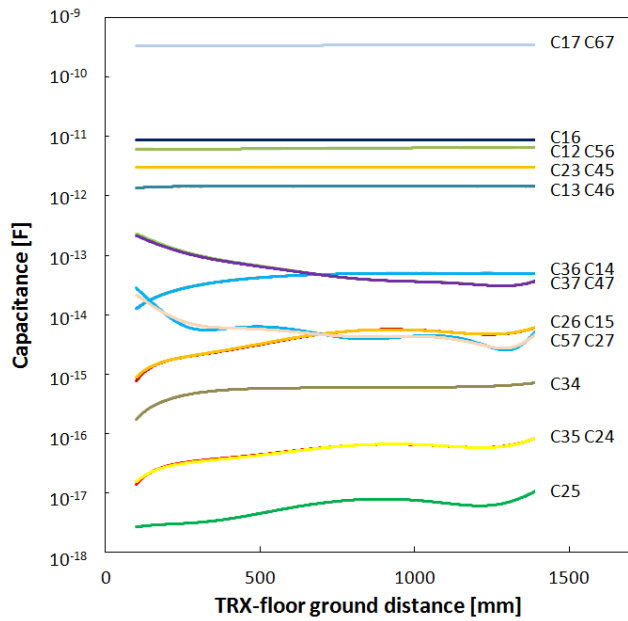


Figure 11. Dependence of capacitance values between seven conductors on the distance between TRX and floor ground in standing posture.

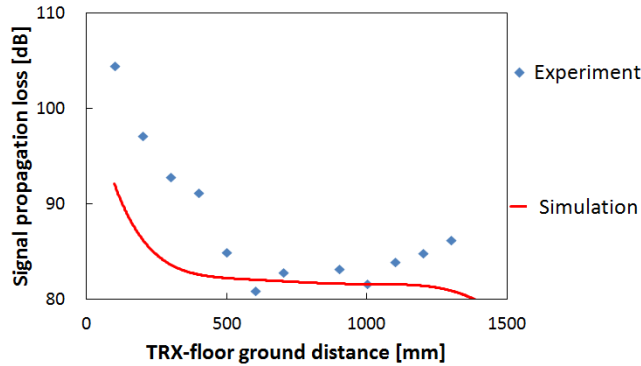


Figure 12. Signal propagation loss as a function of distance between TRX and floor ground in standing posture.

5.3 Handshaking Communication Mechanism

We discuss the signal propagation path from TX to RX to enable handshaking communication based on the equivalent circuit. The coupling force of the capacitive coupling C16 between phantom 1 (no. 1) and phantom 2 (no. 6) was strengthened by handshaking. In order to obtain the signal propagation loss difference between standing posture and handshaking posture, the C16 needs to be a component of the signal propagation path from TX to RX. The currents that flow each capacitance of the equivalent circuit are calculated by circuit simulation. Figure 13 shows the current direction in each capacitance of the equivalent circuit. Figure 14 shows the simulation results of the capacitances as a function of the distance between TRX and floor ground in the standing posture. We investigated the largest outflow currents from each conductor, as shown in Fig. 15. C12, C13, and C23 were components of the signal propagation path. However, because C45 was not a component, this was not a signal propagation path from TX to RX. We therefore proposed two signal propagation

paths from TX to RX composed of C16, C23, and C45 by the largest outflow current from each conductor. If the coupling force of the capacitive coupling C34 was strengthened so as to be $I_{34} > I_{13}$ and the coupling force of the capacitive coupling C16 was strengthened so as to be $I_{16} > I_{67}$, the signal propagation path from the TX to RX follows the path indicated by the red line in Fig. 16. We call the red line signal propagation path 1. If the coupling force of the capacitive coupling C37 was strengthened so as to be $I_{37} > I_{13}$ and the coupling force of the capacitive coupling C47 was strengthened so as to be $I_{47} > I_{17}$, the signal propagation path from the TX to RX follows the path indicated by the green line. We call the green line signal propagation path 2. I67 is larger than I16 in the outflow current from the phantom 2 (no. 6), as shown in Fig. 15. However, I16 is the largest in outflow current from the phantom 2 (no. 6) because the direction of I67 was inverted when the coupling force of the capacitive coupling C37 and C47 was strengthened.

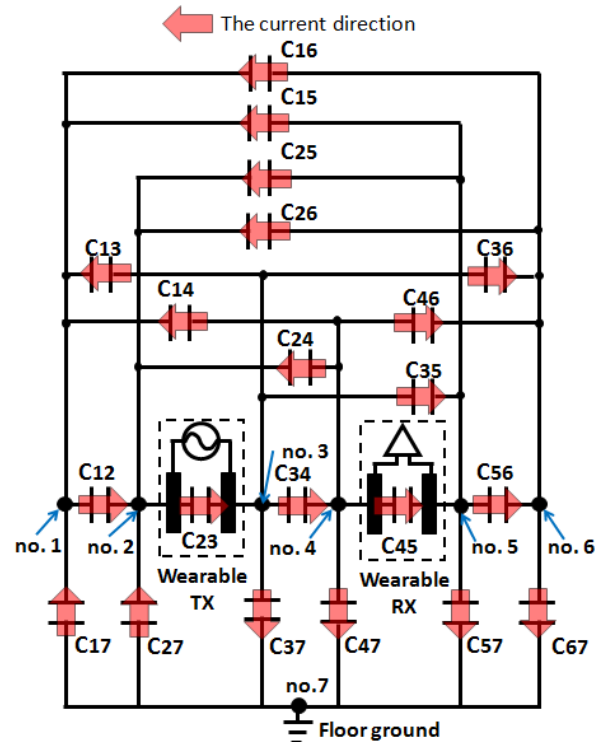


Figure 13. Current direction of the equivalent circuit.

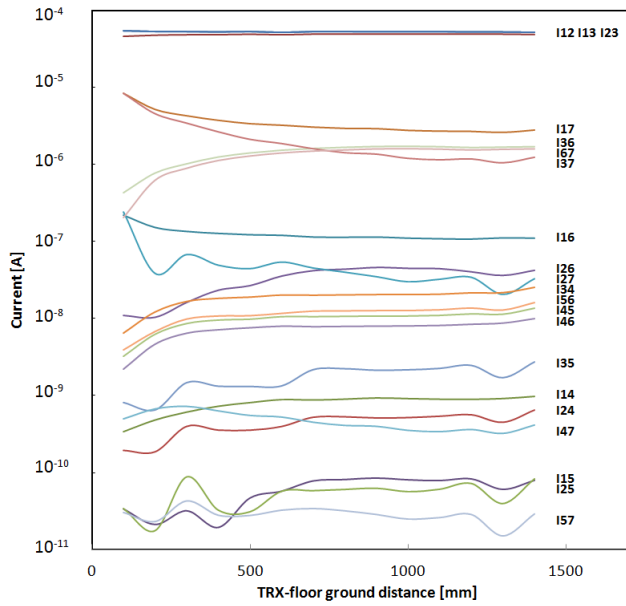


Figure 14. Dependence of current values between seven conductors on the distance between TRX and floor ground in standing posture.

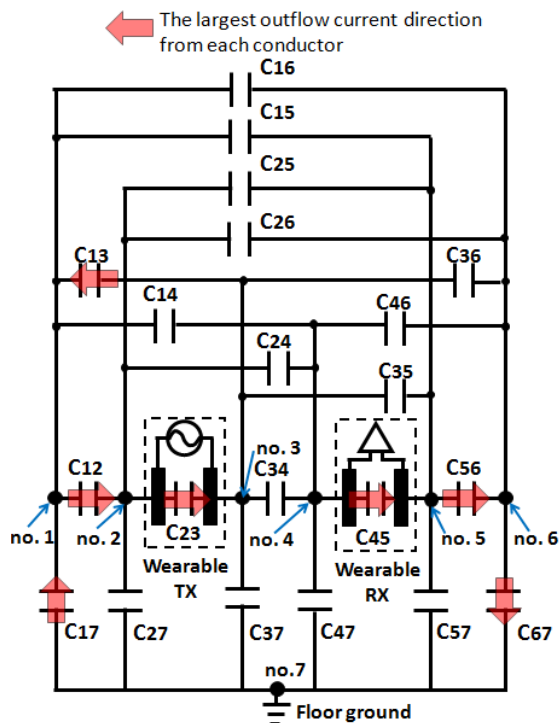


Figure 15. The largest outflow currents direction from each conductor.

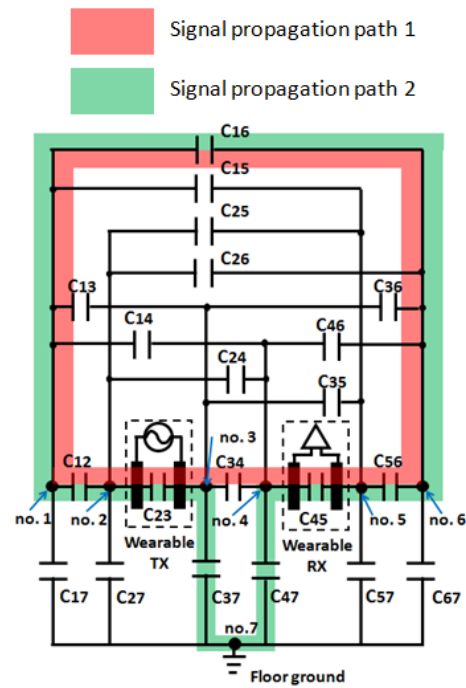


Figure 16. The signal propagation path from TX to RX.

In order to form signal propagation path 1, it is necessary to strengthen the coupling force of the capacitive coupling C34. However, to do so, it is necessary to have a short distance between TRXs and to change the size of TRX, as it is difficult to strengthen the coupling force of the capacitive coupling C34 using the prototype TRX. Handshaking communication does not form the signal propagation path 1. In order to form the signal propagation path 2, it is necessary to strengthen the coupling force of the capacitive coupling C37 and C47. When the distance between TRX and floor ground was short, the coupling force of the capacitive coupling C37 and C47 was strengthened. We propose wearable TRXs that are inserted into the soles of shoes. The schematic of our experimental system with the wearable TRXs in shoe soles is shown in Fig. 17. Also shown is the schematic of our experimental system using an E/O-O/E probe. In this case, we experimentally confirmed that the signal propagation loss in the handshaking posture was smaller than that in the standing posture by 10.6 dB.

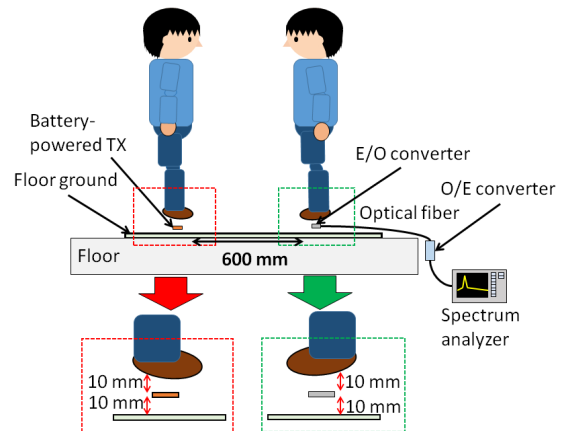


Figure 17. Measurement system when wearable TRXs are inserted into the soles of shoes.

6. CONCLUSION

We discussed the feasibility of handshaking communication between two humans wearing NFCC TRX using the carrier frequency of 6.75 MHz. Signal propagation losses in the standing posture and handshaking posture were measured with an electrically isolated E/O-O/E probe when TRXs were attached to the front of two humans facing each other. In order to clarify the cause of the signal propagation loss difference between the two postures revealed in the experimental results, we investigated the handshaking communication model with simulations using phantoms we developed in place of a real human body. The signal propagation path from TX to RX was revealed by circuit simulation. Finally, we proposed the signal propagation path for the establishment of handshaking communication. When wearable TRXs are inserted into the soles of shoes, the signal propagation path for the establishment of handshaking communication is satisfied. In this case, we experimentally confirmed that the signal propagation loss in handshaking is smaller than that in the standing posture by 10.6 dB, which demonstrates that handshaking communication using current NFCC TRXs can be realized.

ACKNOWLEDGMENTS

Part of this work was supported by a Grant-in-Aid for Scientific Research (A) 23246073 from the Ministry of Education, Culture, Sports, Science and Technology of Japan.

REFERENCES

- [1] Y. Kado and M. Shinagawa. 2011. AC Electric Field Communication for Human-Area Networking. *IEICE Trans. Electron*, vol.E93-C, 234-243.
- [2] T. G. Zimmerman. 1996. Personal Area Networks: Near-field intrabody communication. *IBM System. J*, 35(3/4) 609-617.
- [3] Electric field communication system of the Nippon signal, “elefin” [<http://www.signal.co.jp/products/elefin/>] (accessed 2016- 10-7).
- [4] M. Ishida, T. Nakamura, M. Nozawa, N. Watanabe, Y. Kado, and M. Shinagawa. 2014. MHz-Band RF Signal Propagation Characteristics on Human-Equivalent Phantom for Intra-body Communication. *EuCAP 2014*. 2284-2288.
- [5] M. Ishida, T. Nakamura, M. Nozawa, N. Watanabe, Y. Kado, and M. Shinagawa. 2014. MHz-Band RF Signal Propagation Characteristics on Human Body for Intra-body communication. *I2MTC 2014*. 797-801.
- [6] D. Ayuzawa, N. Sekine, M. Shinagawa, D. Saito, T. Yamada, and K. Oohashi. 2016. Wearable-to-Wearable Device Measurement for Intra-Body Communication Using Electro-Optic Technique. *International Symposium on Optical Memory 2016*. Tu-J-31.
- [7] M. nozawa, T. Nakamura, H. Shimasaki, Y. Kado and M. Shinagawa. 2013. Signal Measurement System Using Electrically Isolated probe for MHz-Band Near-Field Coupling Communication. *IEEE International Instrumentation and Measurement Technology Conference 2013*. 37-40.
- [8] S. Hasegawa, M. Ishida, I. Yokota, Y. Kado, K. Ohashi and D. Saito. 2016. Human body equivalent phantom for analyzing of surface and space propagation in MHz-band signal transmission, *EuCAP 2016*. DOI=<http://dx.doi.org/10.1109/EuCAP.2016.7481823>.
- [9] S. Gabriel, R.W.Lau and C.Gabriel. 1996. The dielectric properties of biological tissues: II .Measurements in the frequency rage 10 Hz to 20 GHz. *Phys. Med. Biol.* 41, 2251-2269.
- [10] N. Haga, K. Motojima, M. Shinagawa and Y. Kado. 2014. System of equations describing charges of multiple conductors immersed in electrostatic fields. *IEICE Electronics Express*. 11, no. 19.
- [11] Y. Hayashida, R. Sugiyama, Y. Ido, A. Suzuki, Y. Takizawa, M. Shinagawa, Y. Kado, and N. Haga. 2014. Capacitance Model of Embedded Transceiver for Intra-body Communication. *BODYNETS 2014*. 222-228.
- [12] S. Hasegawa, I. Yokota, M. Ishida, H. Shimasaki, Y. Kado and M. Shinagawa. 2015. Signal Interference Analysis Model in Near-Field Coupling Communication. *BODYNETS 2015*. 210-215.
- [13] 3D electromagnetic field simulator, “ANSYS Q3D Extractor” [<http://www.ansys.com/Products/Electronics/ANSYS-Q3D-Extractor>] (accessed 2016- 11-18).